Tumor Progression Locus 2 (TPL2) Regulates Obesity-Associated Inflammation and Insulin Resistance

James W. Perfield II,[1] Yunkyoung Lee,[1] Gerald I. Shulman,[2] Varman T. Samuel,[2,3] Michael J. Jurczak,[2] Eugene Chang,[1] Chen Xie,[1] Phillip N. Tsichlis,[4] Martin S. Obin,[1] and Andrew S. Greenberg[1]

OBJECTIVE—Obesity-associated low-grade systemic inflammation resulting from increased adipose mass is strongly related to the development of insulin resistance and type 2 diabetes as well as other metabolic complications. Recent studies have demonstrated that the obese metabolic state can be improved by ablating certain inflammatory signaling pathways. Tumor progression locus 2 (TPL2), a kinase that integrates signals from Toll receptors, cytokine receptors, and inhibitor of κ-B kinase-β is an important regulator of inflammatory pathways. We used TPL2 knockout (KO) mice to investigate the role of TPL2 in mediating obesity-associated inflammation and insulin resistance.

RESEARCH DESIGN AND METHODS—Male TPL2KO and wild-type (WT) littermates were fed a low-fat diet or a high-fat diet to investigate the effect of TPL2 deletion on obesity, inflammation, and insulin sensitivity.

RESULTS—We demonstrate that TPL2 deletion does not alter body weight gain or adipose depot weight. However, hyperinsulinemic euglycemic clamp studies revealed improved insulin sensitivity with enhanced glucose uptake in skeletal muscle and increased suppression of hepatic glucose output in obese TPL2KO mice compared with obese WT mice. Consistent with an improved metabolic phenotype, immune cell infiltration and inflammation was attenuated in the adipose tissue of obese TPL2KO mice coincident with reduced hepatic inflammatory gene expression and lipid accumulation.

CONCLUSIONS—Our results provide the first in vivo demonstration that TPL2 ablation attenuates obesity-associated metabolic dysfunction. These data suggest TPL2 is a novel target for improving the metabolic state associated with obesity. ***Diabetes*** **60:1168–1176, 2011**

Obesity is an independent risk factor for type 2 diabetes, cardiovascular disease, nonalcoholic steatohepatitis, stroke, and certain cancers (1,2). Obesity is now recognized as a state of chronic low-grade systemic inflammation and this inflammatory state promotes the development of obesity-related complications (3–6). Macrophages are a major source of proinflammatory cytokines in adipose tissue and are implicated in the onset and progression of insulin resistance (7–10). Similarly, proinflammatory activation of hepatic macrophages (Kupffer cells) is observed in response to obesogenic diets and is causally implicated in the hepatic and systemic metabolic abnormalities of obesity and type 2 diabetes (11,12). In addition to immune cells, activation of parenchymal cells, including adipocytes and hepatocytes, has been suggested to promote local and systemic insulin resistance with obesity (7–9,13,14).

A current challenge is to identify the mechanisms underlying inflammatory cell recruitment and activation in obese states. Several stimuli have been implicated in promoting the inflammatory profile associated with obesity, including the death of enlarged adipocytes, increased free fatty acid flux, and low-grade systemic endotoxemia (6,13–15). Adipocyte death is associated with infiltration and activation of immune cells in adipose tissue, and endotoxin and fatty acids both activate cell surface receptors such as Toll-like receptors (TLRs) (16).

Recent studies using mouse knockout (KO) models have delineated the importance of several inflammatory signaling pathways in the onset and development of obesity-associated insulin resistance and metabolic dysfunction (7–9,17–21). For example, reduced activation of Jun NH2-terminal kinase (JNK), inhibitor of k-B kinase-β (IKK-β), or TLR4 in immune cells and parenchymal cells has been demonstrated to reduce the systemic inflammation associated with obesity and to improve the metabolic profile. Notably, many of these improvements in metabolic health occurred independent of changes in adiposity (22,23). Accordingly, inflammatory signaling pathways have been targeted for the purposes of preventing or improving obesity-associated insulin resistance (3,9).

Tumor progression locus 2 (TPL2) is a serine/threonine kinase expressed by a variety of cell types that functions downstream of IKK-β and is activated by the tumor necrosis factor (TNF) family of cytokines and cell-associated molecules, interleukin (IL)-1β, several chemokines, and TLR ligands (24,25). The predominate proinflammatory actions of TPL2 depend on the activation of mitogen-activated protein (MAP) kinases, including extracellular signal–related kinase (ERK) and JNK, and upregulated production of cytokines, including TNF-α and IL-1β. The mechanism of TPL2-induced cytokine production has been reported to be specifically by ERK in macrophages and ERK and JNK in nonhematopoietic cells such as fibroblasts and pancreatic cells (26,27). Consistent with these in vitro observations, TPL2KO mice challenged with endotoxin produced dramatically reduced levels of TNF-α protein (28). Overall, ablation of TPL2 blocks the actions

From the [1]Obesity and Metabolism Laboratory, JM-USDA Human Nutrition Research Center on Aging, Tufts University, Boston, Massachusetts; the [2]Departments of Internal Medicine and Cellular & Molecular Physiology, Howard Hughes Medical Institute, Yale University School of Medicine, New Haven, Connecticut; the [3]West Haven VAMC, West Haven, Connecticut; and the [4]Molecular Oncology Research Institute, Tufts University School of Medicine, Boston, Massachusetts.

Corresponding author: Andrew S. Greenberg, andrew.greenberg@tufts.edu, or Martin S. Obin, martin.obin@tufts.edu.

Received 19 May 2010 and accepted 24 January 2011.

DOI: 10.2337/db10-0715

This article contains Supplementary Data online at http://diabetes.diabetesjournals.org/lookup/suppl/doi:10.2337/db10-0715/-/DC1.

J.W.P. and Y.L. contributed equally to this study.

J.W.P. is currently affiliated with the Departments of Nutrition & Exercise Physiology and Food Science, University of Missouri, Columbia, Missouri.

of cytokines (TNF-α and IL-1β) and proinflammatory stimuli (lipopolysaccharide) to activate ERK, and in certain cell types, JNK (29,30). Thus, TPL2 is uniquely positioned to integrate the multiple inflammatory signaling pathways implicated in the development and progression of obesity-associated complications. TPL2 expression was recently reported to be upregulated in obese adipose tissue, further supporting the notion that TPL2 is a potential mediator of obesity-associated inflammation (31). However, in vivo studies examining the role of TPL2 in obesity and its associated metabolic disorders are lacking.

The current study used TPL2KO and wild-type (WT) mice to investigate TPL2 in high-fat diet (HFD)-induced obesity, inflammation, and insulin resistance. We demonstrate that lack of TPL2 reduces HFD-induced macrophage recruitment, mitogen-activated protein kinase (MAPK) activation, and inflammatory gene expression in adipose tissue and liver, improves insulin signaling and sensitivity, and attenuates lipopolysaccharide-induced inflammatory gene expression in bone marrow–derived macrophages (BMDMs). The salutary effects on inflammation and metabolism are observed in the absence of a significant effect of TPL2 ablation on body weight or adipose mass. These data are the first to demonstrate a role for TPL2 in obesity-associated metabolic dysfunction and suggest that TPL2 is a novel target for regulating the development and metabolic impacts of obesity-associated inflammation.

RESEARCH DESIGN AND METHODS

Materials. Human insulin (Novolin R) and recombinant macrophage colony stimulating factor (M-CSF) were purchased from Novo Nordisk (Denmark) and enScript (Piscataway, NJ), respectively. Antibodies recognizing ERK (9102), phospho-ERK (9101), JNK (9252), phospho-JNK (9251), AKT (9272), and phospho-Akt (9271) were obtained from Cell Signaling (Danvers, MA), and a MAC-2 (CL8942AP) antibody was obtained from Cedarlane (Burlington, ON, Canada). Horseradish peroxidase-conjugated secondary antibodies and bicinchoninic acid protein assay reagents were obtained from Thermo Scientific (Rockford, IL). Enhanced chemiluminescence reagent was purchased from PerkinElmer Life Sciences (Boston, MA). Immunohistochemistry was performed by VectaStain Elite ABC kit (Vecta Laboratory, Burlingame, CA). Cell culture products were obtained from Gibco (Carlsbad, CA), and chemical reagents were purchased from Sigma-Aldrich (St. Louis, MO).

Isolation of BMD cells. Bone-marrow cells were isolated from femoral and tibial bone marrow of WT and TPL2KO mice and differentiated to macrophages in the presence of M-CSF (17,32). Media for the culture of BMDM was composed of 80% DMEM, 20% heat-inactivated FBS, 2.0 g/L glucose, 100 μmol/L nonessential amino acid, 2 mmol/L L-glutamine, 100 ng/mL M-CSF, and penicillin/streptomycin. The progenitor cells were proliferated and differentiated to mature macrophages for 5 days, at which point adherent viable cells were harvested and plated in six-well plates.

Animals and diets. Experiments were conducted in a viral pathogen–free facility at the Jean Mayer-U.S. Department of Agriculture Human Nutrition Research Center on Aging at Tufts University in accordance with Institutional Animal Care and Use Committee guidelines. WT and TPL2KO mice generated from heterozygous matings were used as homozygous breeding pairs to generate WT and KO experimental mice. Genotyping of animals was verified at weaning and again when mice were killed. Male 6-week-old mice were individually caged and fed a normal diet (ND) with 17% calories from fat (Harlan #7012) or HFD with 60% calories from fat (Research Diets D12492) for 17 weeks. Mice were killed by CO_2 narcosis, followed by cardiac puncture. Tissues were dissected, weighed, and snap frozen for analysis of protein or gene expression, or were fixed, embedded in paraffin, and sectioned for histologic analysis.

Measures of insulin resistance and signaling. Fasted (overnight) plasma insulin was measured by ELISA (Crystal Chem, Downers Grove, IL). A hyperinsulinemic-euglycemic clamp was performed for 120 minutes, after an overnight fast, using a primed/continuous infusion of human insulin (126 pmol/kg prime, 18 pmol/kg/min infusion) as described (33). During the clamp, plasma glucose was maintained at basal concentrations. Rates of basal and insulin-stimulated whole-body glucose fluxes and tissue glucose uptake were determined as described (33). To assess peripheral tissue insulin sensitivity, mice were fasted 6 h and then received an intraperitoneal injection of saline (basal) or insulin (stimulated, 0.75 μU/kg). Mice were killed 10 minutes after injection, and blood and adipose, liver, and muscle tissues were collected and snap frozen until Western blotting analyses.

Western blotting analysis. Protein from the frozen tissue samples was isolated as described previously (34). Briefly, gonadal adipose and liver were processed in 5% SDS lysis buffer and muscle was pulverized in liquid nitrogen and processed in a 1% Triton X-100 buffer. Proteins were separated by SDS-PAGE and transferred to Hybond enhanced chemiluminescence nitrocellulose membrane and incubated with the indicated antibody and horseradish peroxidase-coupled anti-species antibodies. Proteins were visualized by enhanced chemiluminescence and quantified by densitometry.

RNA isolation, reverse transcription, and real-time quantitative PCR. Adipose tissue RNA was extracted using Qiagen Lipid Mini kits and liver RNA was isolated using Qiagen Mini kits according to manufacturer's instructions. RNA was quantified and checked for purity using the Nanodrop spectrophotometer (Nanodrop 1000, Wilmington, DE). cDNA was generated from 1 μg of RNA, and real-time quantitative PCR was performed using SYBR Green (Applied Biosystems 7300, Carlsbad, CA). Fold-changes were calculated as $2^{-\Delta\Delta CT}$, with cyclophilin A or cyclophilin B used as the endogenous control.

Liver triglyceride. Liver triglyceride content was determined using a modified protocol described by Schwartz and Wolins (35). Briefly, frozen liver was extracted in PBS-10 mmol/L EDTA buffer, and protein concentration was determined by bicinchoninic acid protein assay. Samples were assayed in duplicate, and 25 μg of protein extract was subjected to organic extraction. Triglyceride was quantified using a colorimetric enzyme-linked kit (Sigma).

Immunohistochemistry. Gonadal adipose and liver tissue were fixed in 4% formaldehyde overnight, embedded in paraffin, sectioned, and stained with hematoxylin and eosin (H&E). Digital images were acquired with an Olympus DX51 light microscope (Center Valley, PA). Adipocyte death was quantified by identification of crown-like structures (CLS) within histologic sections of epididymal adipose tissue. The percentage of CLS ([number dead adipocytes/number total adipocytes] × 100) was calculated and used for comparison among experimental groups. Adipocyte volume was calculated from cross-sectional area obtained from perimeter tracings using Image J software (Sun Microsystems, Santa Clara, CA) (13).

Statistical analysis. Data are presented as mean ± SE. Data were determined to have a normal distribution with equal variance, and statistical differences were determined by *t* test or ANOVA using the Tukey least significant differences test for post hoc determination using Minitab software (University Park, PA). Significance was set at $P \leq 0.05$.

RESULTS

The effect of TPL2 deletion on diet-induced obesity. The 6-week-old male TPL2KO and WT mice were fed ND or HFD for 17 weeks. Although the HFD increased growth rate and final body weight compared with the ND, we observed no difference in these variables between WT and TPL2KO mice receiving the same diet (Supplementary Fig. 1 and Table 1). Consistent with a lack of difference in body weight, food intake and fat pad mass were similar between obese WT and TPL2KO mice (Table 1). We did observe a small but significant reduction in the liver weight of TPL2KO mice fed an HFD. Obesity is typically associated with decreased insulin sensitivity and elevated circulating concentrations of glucose and insulin. Despite having a similar body weight and fat pad mass, 6-h fasting blood glucose and overnight fasting plasma insulin concentrations were decreased in obese TPL2KO mice, suggesting an improved insulin sensitivity, which is further investigated subsequently. Although we did not observe a difference in blood glucose concentrations after an overnight fast (data not shown), a recent report indicated that in mice, blood glucose concentrations after a 6-h fast are a better representation of blood glucose levels throughout the day (36).

Consistent with an improved metabolic state, obese TPL2KO mice had reduced plasma concentrations of the proinflammatory cytokines TNF-α and IL-6 (Supplementary Table 1). Plasma concentrations of nonesterified fatty acid, leptin, and resistin were not significantly different between

TABLE 1
Metabolic parameters of WT and TPL2KO mice

Parameters	ND		HFD	
	WT	TPL2KO	WT	TPL2KO
Body wt (g)	26.54 ± 0.87	28.54 ± 0.25	41.35 ± 0.86	41.22 ± 1.17
Food intake (g)	4.24 ± 0.27	4.29 ± 0.34	2.80 ± 0.13	2.73 ± 0.06
Liver (g)	1.02 ± 0.09	1.11 ± 0.06*	1.29 ± 0.05	1.18 ± 0.05*
Subcutaneous fat (g)	0.22 ± 0.04	0.31 ± 0.04	1.96 ± 0.18	2.37 ± 0.30
Gonadal fat (g)	0.38 ± 0.09	0.40 ± 0.04	2.29 ± 0.15	2.31 ± 0.20
Fasting glucose (mg/dL)†	205.67 ± 11.32	182.50 ± 12.97	257.50 ± 14.33	213.17 ± 11.06*
Fasting insulin (ng/mL)‡	0.46 ± 0.15	0.64 ± 0.16	2.52 ± 0.40	1.43 ± 0.21*

WT and TPL2KO mice were fed an ND or an HFD for 17 weeks, and plasma was collected as described in RESEARCH DESIGN AND METHODS (n = 5–6 mice per group). *Indicates a statistical difference within a dietary treatment group ($P < 0.05$). †Fasting glucose concentrations were measured from 6-h fasted mice. ‡Fasting insulin concentrations were measured from plasma collected after an overnight fast.

obese WT and TPL2KO mice (Supplementary Table 1). We observed no differences in plasma glucose, insulin, or proinflammatory cytokine concentrations in ND-fed WT and TPL2KO mice (data not shown). In summary, obese TPL2KO mice had reduced levels of circulating cytokines and improvements in glucose-insulin homeostasis compared with obese WT mice.

TPL2 regulates immune cell infiltration and inflammation in obese adipose tissue. TPL2 is located downstream of IKK-β and regulates MAPK activation, both of which have been implicated in obesity-associated inflammation. Therefore, we investigated the effects of TPL2 ablation on adipose tissue inflammation. A hallmark of obesity-associated adipose tissue inflammation is the localization of macrophages around dead adipocytes to form CLS (6,13). Importantly, the presence of CLS in the adipose tissue of obese TPL2KO mice was reduced by more than 70% (Fig. 1*A* and *C*). The observed reduction in CLS occurred independent of a difference in adipocyte size (Fig. 1*B*) or fat pad mass (Table 1). Consistent with the observed reduction in CLS, gene expression of the general macrophage marker *F4/80* was attenuated in the adipose tissue of obese TPL2KO mice (Fig. 2). We observed a similar reduction in the expression of *CD11c*, a marker for a subset of proinflammatory immune cells that have been demonstrated to be major contributors to the insulin resistance associated with obesity (17,32). In accordance with a reduced inflammatory phenotype, relative mRNA expression of the cytokine *TNF-α* and the chemokine monocyte chemoattractant protein-1 (*MCP-1*) were also markedly reduced in obese TPL2KO adipose tissue.

Gene expression of *TLR2* and *TLR4* was upregulated with obesity in WT mice, and this increase was diminished in obese TPL2KO mice (Fig. 2). Furthermore, lack of TPL2 signaling in adipose tissue attenuated obesity-induced activation of ERK and JNK, which is consistent with our observation of reduced inflammatory gene expression (Fig. 3). In summary, the adipose tissue of obese TPL2KO mice had significantly reduced immune cell infiltration, MAPK signaling, and inflammatory mediators that have been implicated in local and systemic insulin resistance.

TPL2 deficiency reduces obesity-induced liver steatosis and inflammation. Increased hepatic inflammation and steatosis are prominent characteristics of obesity and are risk factors for the development of insulin resistance. Histology suggested that livers of obese WT mice contained more lipid than livers of obese TPL2KO mice (Fig. 4*A*), and analysis by organic extraction confirmed liver triglyceride content was 30% greater in obese WT mice (Fig. 4*B*). This reduction in liver triglyceride may explain the small reduction in liver weight observed between obese WT and TPL2KO mice (Table 1). Consistent with our observed differences in liver triglyceride values, several genes associated with lipogenesis and lipid storage, such as *PPARγ*, *GPAT*, and *ADRP*, were significantly decreased in the livers of obese TPL2KO mice compared with their obese WT counterparts (Fig. 4*C*). Additional analysis of the livers revealed reduced gene expression of macrophage markers (*CD11b*, *CD11c*), *TLR2*, and the cytokines *TNF-α* and *IL-6* in the obese TPL2KO mice compared with obese WT controls (Fig. 4*D*).

We also observed a reduction in suppressor of cytokine signaling (*SOCS*)*-1* expression and a trend for reduced *SOCS-3* expression in obese TPL2KO mice. These data support the notion of an improved liver phenotype, because research has shown expression of *SOCS-1* and *SOCS-3* is increased in the livers of obese insulin-resistant animals (37,38).

We did not observe an effect of obesity or lack of TPL2 signaling on activation of ERK and JNK in the liver (Supplementary Fig. 2). However, these studies examined ERK and JNK activation in the entire liver, not in specific cell types, such as macrophages or Kupffer cells, in which there may have been an effect. Overall, obese TPL2KO mice have reduced triglyceride accumulation in their livers, reduced expression of *SOCS*, and decreased mRNA expression of lipogenic and inflammatory genes.

BMDM devoid of TPL2 have a reduced inflammatory phenotype. It is generally well accepted that BMD immune cells contribute significantly to the inflammation that occurs with obesity (4,39). Systemic concentrations of fatty acids and endotoxin (lipopolysaccharide) are increased with obesity and are able to induce an inflammatory response through TLR4 activation (16). To better understand our observation of reduced inflammation in obese TPL2KO mice, we cultured BMDM from WT and TPL2KO mice to determine the consequences of TLR activation. Macrophages from WT and TPL2KO mice were differentiated and treated with or without the TLR agonist lipopolysaccharide for 3 h. We observed that in response to lipopolysaccharide treatment, TPL2KO BMDM expressed significantly less *TNF-α*, *IL-6*, and *MCP-1* mRNA compared with BMDM isolated from WT mice (Fig. 5*A*). Consistent with the gene expression data, TPL2KO BMDM secreted less TNF-α and IL-6 protein, and there was a trend for reduced MCP-1 secretion (Fig. 5*B*). The difference in secreted TNF-α between WT and TPL2KO macrophages was significantly more robust than the difference in *TNF-α* mRNA, a finding

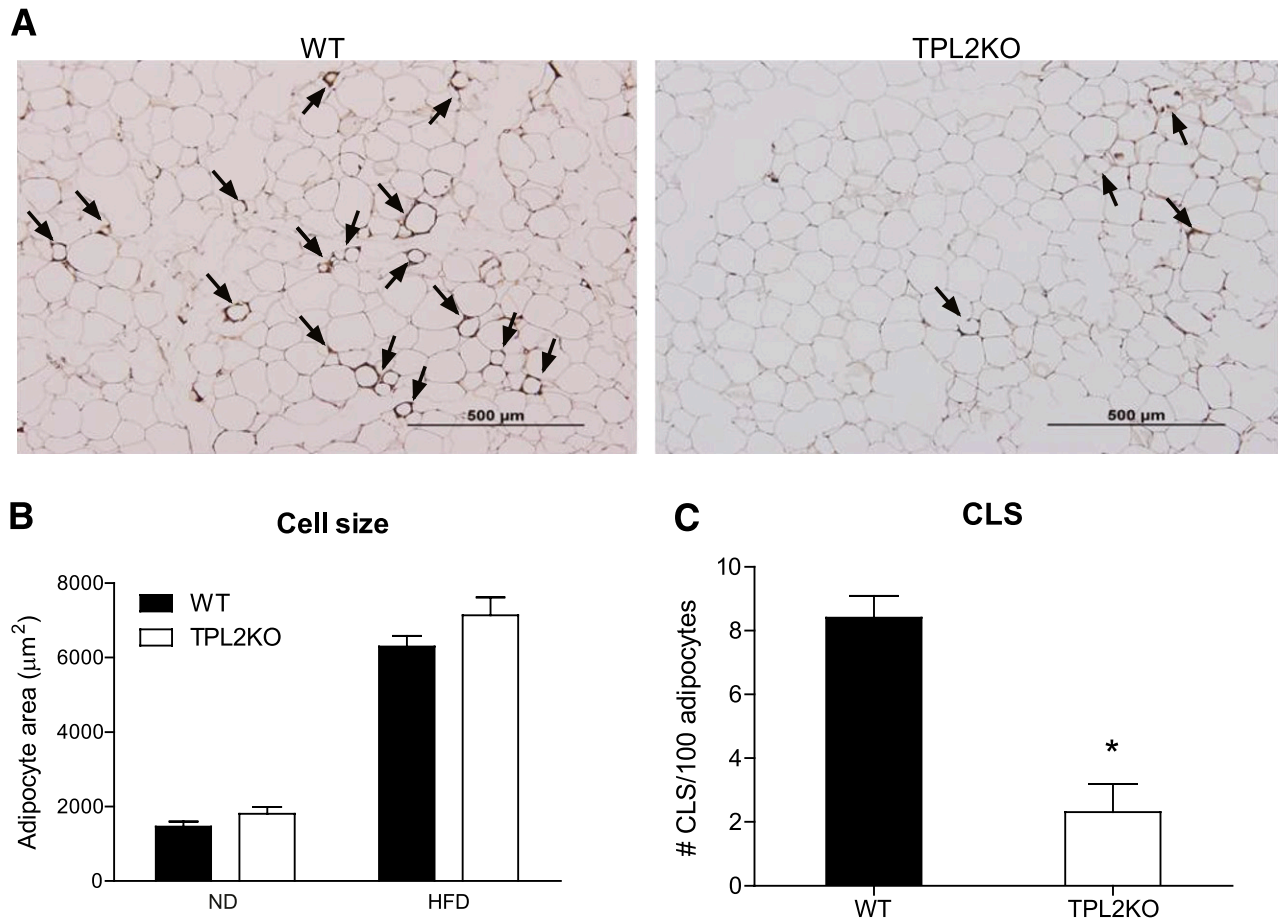

FIG. 1. TPL2 ablation reduces macrophage accumulation in obese adipose tissue. *A*: MAC-2 immunohistochemistry of gonadal adipose tissue from obese WT (*left panel*) and TPL2KO mice (*right panel*); the *black arrows* indicate a CLS. *B*: Average size of adipocytes within gonadal adipose tissue ($n = 5$). *C*: Quantification of CLS from multiple histologic sections ($n = 5$). *$P < 0.05$. Mean data are shown with the SE (*error bars*). (A high-quality color representation of this figure is available in the online issue.)

consistent with a role for TPL2 in the post-transcriptional regulation of this cytokine (28). In the absence of lipopolysaccharide stimulation, basal secretion of these factors was below the minimum detectable limits of the assays (data not shown). These in vitro studies are consistent with our in vivo observations and confirm a role for TPL2 in modulating the expression of cytokines and chemokines in response to an inflammatory stimulus.

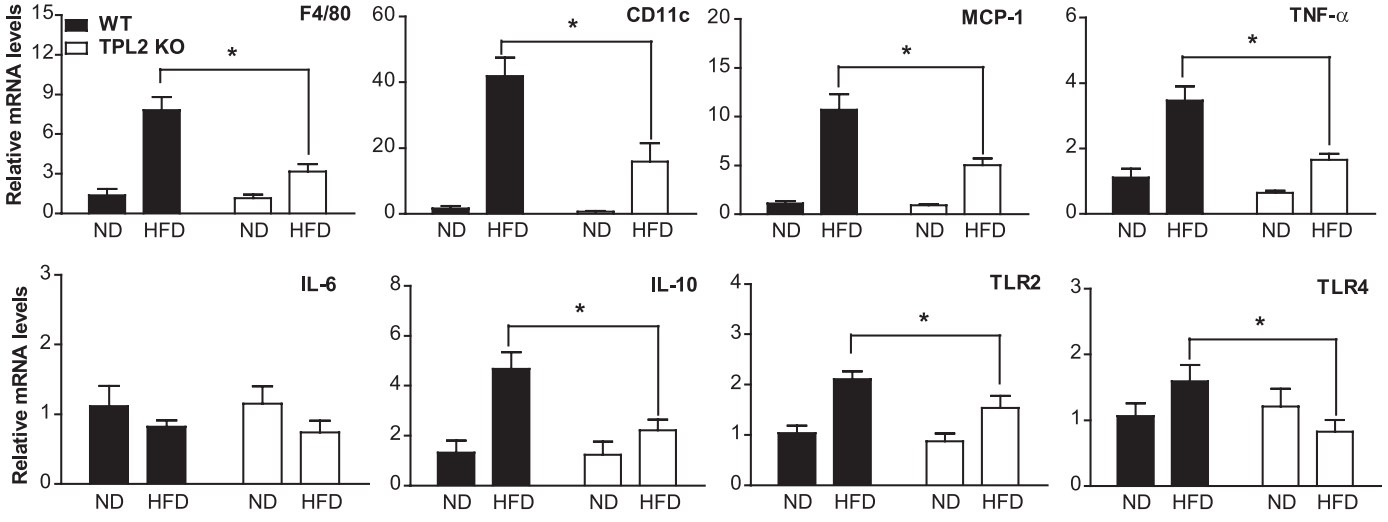

FIG. 2. Obesity-induced inflammation is attenuated in the adipose tissue of TPL2KO mice. Relative mRNA expression of macrophage and inflammatory markers in gonadal adipose tissue from WT or TPL2KO mice fed an ND or an HFD ($n = 5$–6). *$P < 0.05$. Mean data are shown with the SE (*error bars*).

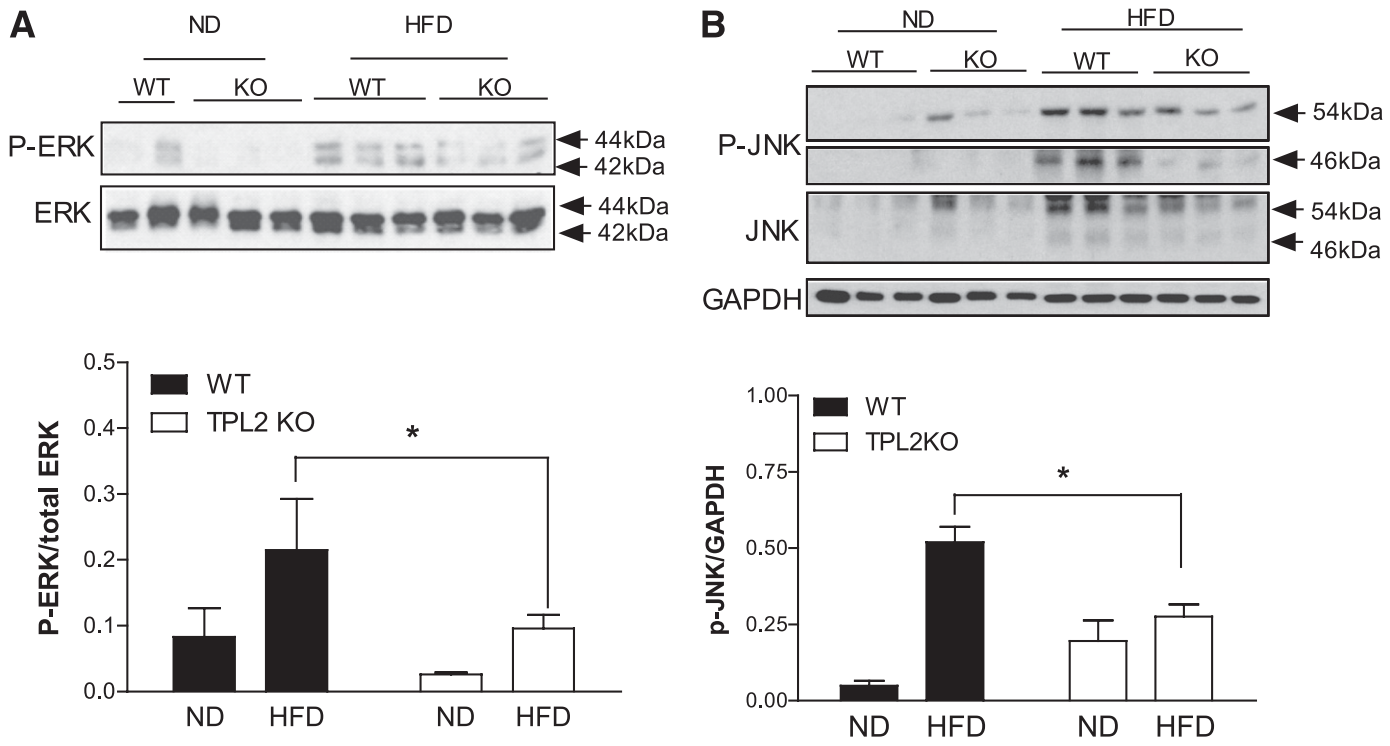

FIG. 3. Lack of TPL2 signaling diminishes obesity-induced activation of ERK and JNK in gonadal adipose tissue. Representative immunoblot analysis of phospho-ERK (Thr202/Tyr204) and total ERK (*A*), phospho-JNK (Thr183/Tyr185) and total JNK (*B*) in gonadal adipose tissue of WT or TPL2KO mice fed an ND or an HFD (n = 2–3). Intensity of phospho-JNK was normalized to total JNK and glyceraldehyde-3-phosphate dehydrogenase (GAPDH) to account for apparent differences in total JNK and confirm statistical significance. *$P < 0.05$. Mean data are shown with the SE (*error bars*).

Improved insulin sensitivity in obese TPL2KO mice. To determine the physiologic consequences of TPL2 ablation on glucose-insulin homeostasis in obese mice, we performed hyperinsulinemic euglycemic clamps on obese WT and TPL2KO mice (Fig. 6; Supplementary Table 2). The infusion rate of exogenous glucose during the clamp was approximately 100% greater in obese TPL2KO mice (22.7 ± 2 mg/kg/min) compared with obese WT mice (11.6 ± 1.6 mg/kg/min; Fig. 6*B*; Supplementary Table 2). This enhanced insulin sensitivity in obese TPL2KO mice reflects enhanced insulin suppression of hepatic glucose output (89% suppression in obese TPL2KO compared with 30% in obese WT; Fig. 6*C*) as well as enhanced insulin-stimulated whole-body glucose uptake (Fig. 6*D*; Supplementary Table 2). The latter is reflected in the enhanced insulin-stimulated glucose uptake in skeletal muscle, which was significantly (80%) increased in obese TPL2KO mice compared with obese WT mice (Fig. 6*E*). In contrast with its salutary effects on liver and muscle insulin sensitivity, TPL2 ablation had no effect on insulin-stimulated glucose uptake in adipose tissue (Fig. 6*E*).

We next asked if enhanced hepatic and skeletal muscle insulin sensitivity in obese TPL2KO mice was associated with enhanced insulin signaling, measured as the magnitude of Akt phosphorylation in response to an insulin bolus. Insulin-stimulated Akt phosphorylation was greater in skeletal muscle and adipose tissue of obese TPL2KO mice than in obese WT mice, whereas liver Akt was activated to a similar extent regardless of TPL2 status (Supplementary Fig. 3). Inflammatory gene expression and ectopic triglyceride/metabolite accumulation are both implicated in the compromised peripheral insulin signaling of obesity (40,41). In the current study, enhanced Akt phosphorylation in skeletal muscle of TPL2KO mice was not associated with significantly reduced skeletal muscle inflammatory gene expression (data not shown) but did correlate with a significant reduction in triglyceride content compared with obese WT mice (Supplementary Fig. 4). Interestingly, reduced muscle triglyceride in obese TL2KO mice was observed in the absence of reduced basal or insulin-suppressed plasma free fatty acids (data not shown; see DISCUSSION).

In summary, these studies provide strong evidence of a protected metabolic phenotype in obese TPL2KO mice and are consistent with our data demonstrating decreases in local and systemic inflammation and reduced accumulation of triglyceride in liver and skeletal muscle.

DISCUSSION

The serine/threonine kinase TPL2 integrates inflammatory inputs from the MAP kinase and IKK/NF-κB signaling pathways (24–26) and is upregulated in the inflamed adipose tissue of obese mice and humans (31). These observations suggest that TPL2 actions promote the inflammatory and metabolic complications of obesity. The current study used a diet-induced obesity paradigm with TPL2KO and WT mice to provide the first demonstration that TPL2 deletion reduces peripheral inflammation, hepatic steatosis, and improves whole-body insulin resistance in the obese state. A key finding of our study was that whole-body insulin sensitivity was improved in obese TPL2KO mice compared with obese WT controls. The observed improvement in glucose-insulin homeostasis was due to increased glucose uptake in skeletal muscle and also increased suppression of hepatic glucose output.

Importantly, the improvement in whole body insulin sensitivity in obese TPL2KO mice occurred in the absence

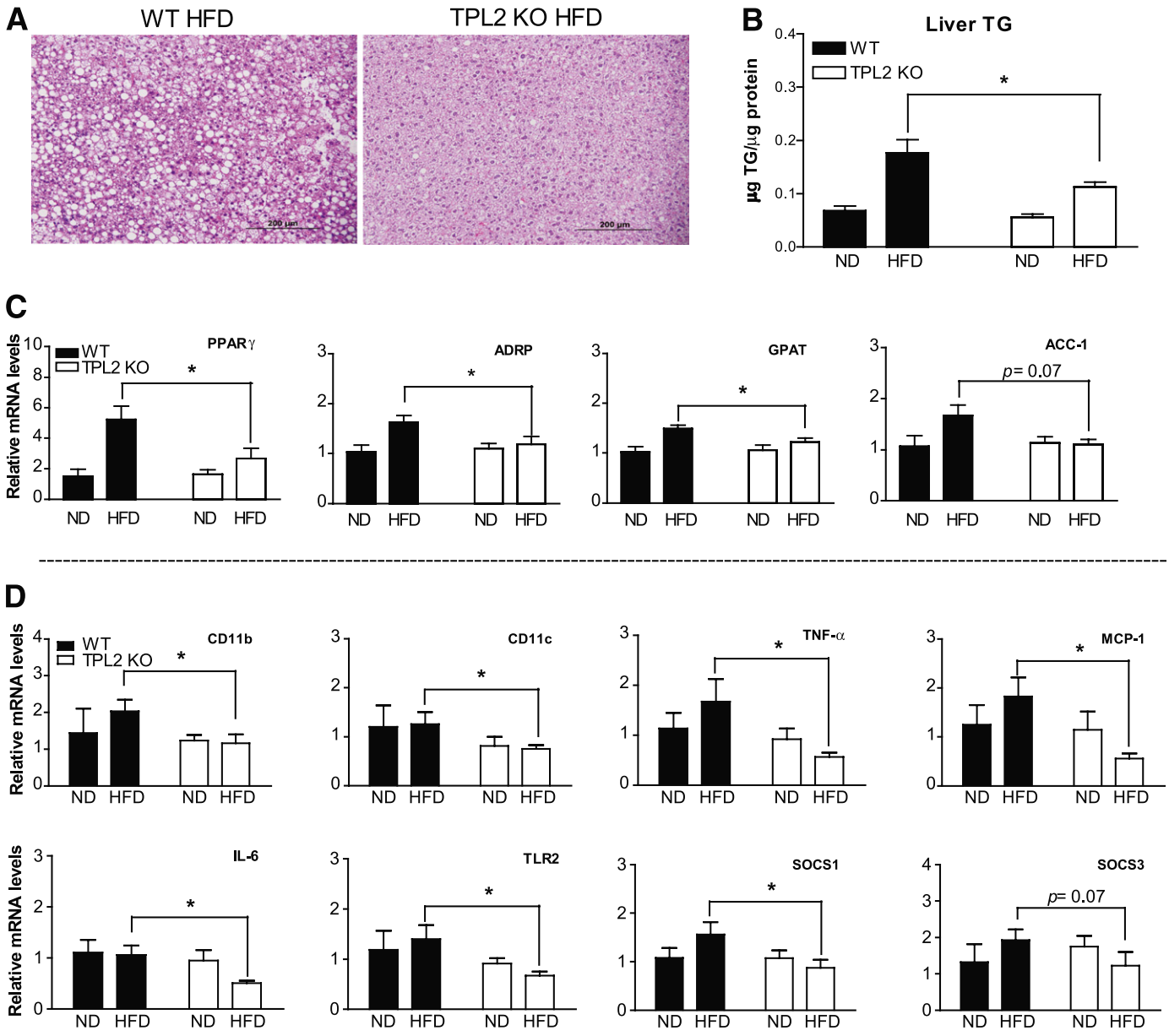

FIG. 4. TPL2 deficiency reduces obesity-induced liver inflammation and steatosis. *A*: Representative H&E stain of liver from the obese WT (*left*) and TPL2KO (*right*) mice. *B*: Liver triglyceride (TG) content of WT or TPL2KO mice fed an ND or an HFD. *C* and *D*: Relative gene expression of lipogenic genes and inflammatory markers in livers from WT or TPL2KO mice fed an ND or an HFD (n = 5–6). *$P < 0.05$. Mean data are shown with the SE (*error bars*). (A high-quality color representation of this figure is available in the online issue.)

of any reductions in adipose depot mass, suggesting that an alternative mechanism promotes enhanced insulin sensitivity in TPL2KO mice. Specifically, our results suggest that the improved metabolic profile of TPL2KO mice reflects the salutary effects of *TPL2* gene ablation on inflammation.

Two key components of the TPL2-mediated signaling axis in nonhematopoetic and hematopoietic cells and tissues are the MAP kinases ERK and JNK (26,27), both of which are implicated in obesity-associated insulin resistance. JNK and ERK activity are both increased in adipocytes from obese patients with diabetes, and this MAPK activation has been linked to the development of insulin resistance, either directly or indirectly, by increased production of downstream inflammatory mediators such as TNF-α and IL-6 (8,42). Phosphorylation of both JNK and ERK was increased in the adipose tissue of WT mice in response to diet-induced obesity, and this increase was attenuated by ≥50% in TPL2KO mice.

Adipose tissue inflammation is largely due to the proinflammatory actions of recruited BMD immune cells (4–6). In both rodents and humans (43–45), the metabolic complications of obesity are associated with the accumulation of proinflammatory macrophages ($F4/80^+$ cells) that express the dendritic cell marker CD11c in adipose tissue (13,46). These macrophages selectively localize to CLS surrounding dead and dying adipocytes (6). Genetic ablation of $CD11c^+$ cells results in significant reductions in CLS and improves metabolic profiles in obese mice (17,45). Our data suggest that TPL2 is a key regulator of $CD11c^+$ macrophage infiltration and inflammation in obese adipose tissue. Gene expression of *F4/80* and *CD11c* were dramatically decreased in the adipose tissue of obese TPL2KO

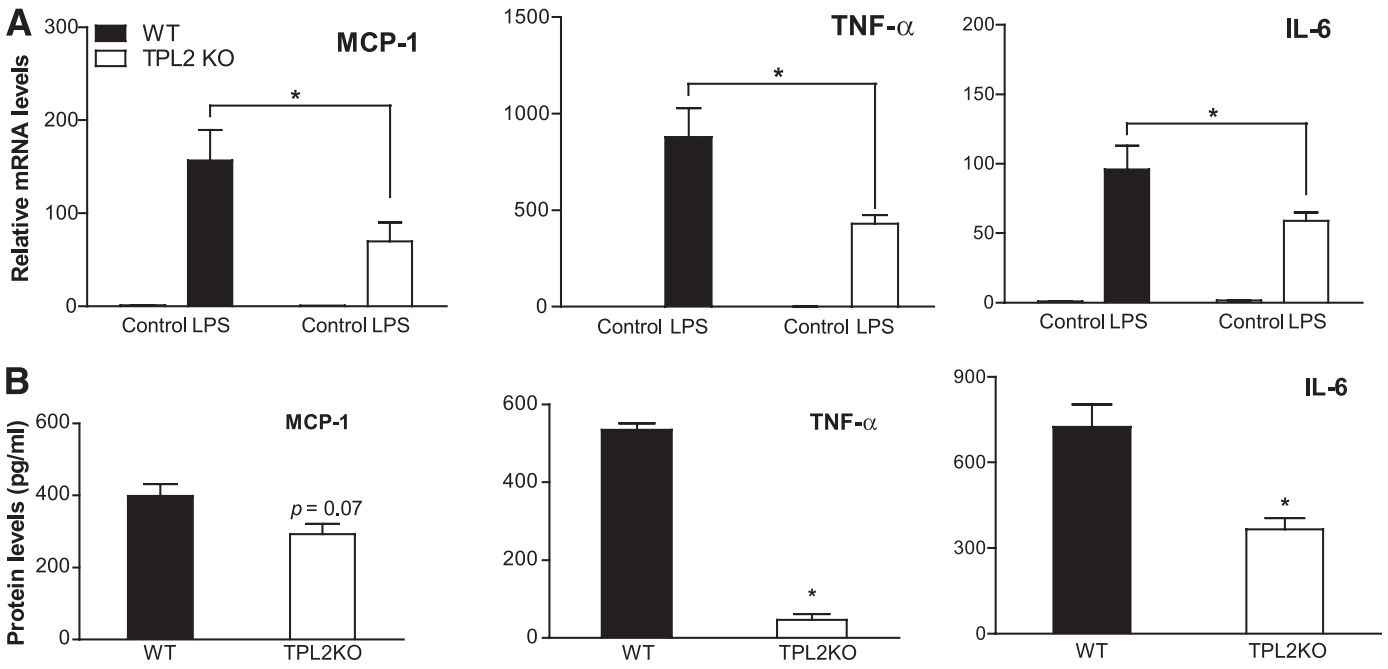

FIG. 5. TPL2KO BMDMs have a reduced inflammatory phenotype. *A*: Relative gene expression (fold change) of inflammatory cytokines and chemokine in BMDM from WT and TPL2KO mice that were simulated with or without lipopolysaccharide (LPS; 100 ng/mL) for 3 h. *B*: Protein concentrations in the culture media were measured by enzyme-linked immunosorbent assay (data are the average of three separate experiments performed in duplicate). *$P < 0.05$. The *error bars* designate the SE.

mice, suggesting reduced infiltration or retention of $CD11c^+$ macrophages. Consistent with this observation, the frequency of CLS and mRNA levels of *MCP-1* and *TNF-α* were both significantly reduced. Our data do not rule out the possibility that reduced adipose tissue inflammation in TPL2KO mice reflects altered inflammatory responses of T-cells (47) or other adipose tissue immune cells.

TPL2 is a master regulator of ERK-dependent gene expression downstream of TLRs in hematopoietic cells, including macrophages (25,48). Thus, in addition to its effects on adipose tissue macrophage recruitment, TPL2 ablation is likely to have direct effects on macrophage inflammatory gene expression in obesity. We therefore determined the effect of TPL2 ablation on lipopolysaccharide-induced *IL-6*, *MCP-1*, and *TNF-α* expression in BMDM from WT and TPL2KO mice. We observed reduced secretion of TNFα, MCP-1, and IL-6 from TPL2KO BMDM. These data are in line with the gene expression data from the adipose tissue or liver, or both, of obese WT and TPL2KO mice and suggest TPL2 signaling in immune cells is an important factor in the initiation and maintenance of obesity-induced peripheral inflammation.

In addition to reducing adipose tissue immune cell infiltration and inflammation, ablation of TPL2 signaling in obese mice reduced hepatic lipid accumulation and inflammation. Decreased hepatic inflammation and lipid accumulation are both associated with improved insulin action in the liver. Hepatic inflammation is linked to enhanced triglyceride deposition in the liver; therefore, TPL2 ablation may reduce hepatic steatosis by directly reducing hepatic inflammation, for example, in Kupffer cells.

Alternatively our observations are consistent with studies reporting positive associations between visceral adipose tissue inflammation and hepatic inflammation in obese humans (49) and mice (13). Future studies using tissue-specific TPL2 ablation will be required to determine if the observed reduction in hepatic inflammation is a result of reduced adipose tissue inflammation or is caused by a lack of TPL2 signaling in the liver.

Accumulation of triglyceride and active lipid species (i.e., diacylglycerols) has been implicated in the pathogenesis of insulin resistance (40,41) and could be a common denominator in the improved metabolic profile observed in liver and muscle. Triglyceride accumulation was reduced in the liver and skeletal muscle in obese TPL2KO mice compared with obese WT mice. Consistent with reduced ectopic triglyceride accumulation, the clamp studies demonstrated increased sensitivity to insulin's actions in liver and skeletal muscle. Insulin-stimulated Akt phosphorylation was enhanced in skeletal muscle but not in the liver of obese TPL2KO mice. This discrepancy between clamp and Akt data presumably reflects differential responses to an acute insulin bolus versus the integrated physiologic response to a steady-state insulin infusion during the clamp. It is intriguing that reduced ectopic triglyceride was observed in obese TPL2KO mice without a relative reduction in basal or clamped plasma free fatty acid concentrations. Future studies will address the mechanism(s) by which TPL2 reduces ectopic triglyceride accumulation in the liver and skeletal muscle and its role in improving glucose-insulin homeostasis.

In summary, the current study demonstrates a significant role for TPL2 in obesity-induced inflammation and metabolic dysfunction. TPL2 deletion in the obese state prevents MAPK activation, proinflammatory cytokine expression, and the accumulation of immune cells in peripheral tissues, resulting in reduced hepatic steatosis and improved insulin sensitivity. The recent report of increased TPL2 activity in human obesity (31) and the results of the current study suggest that TPL2 is a promising therapeutic target for the inflammatory and metabolic complications of obesity.

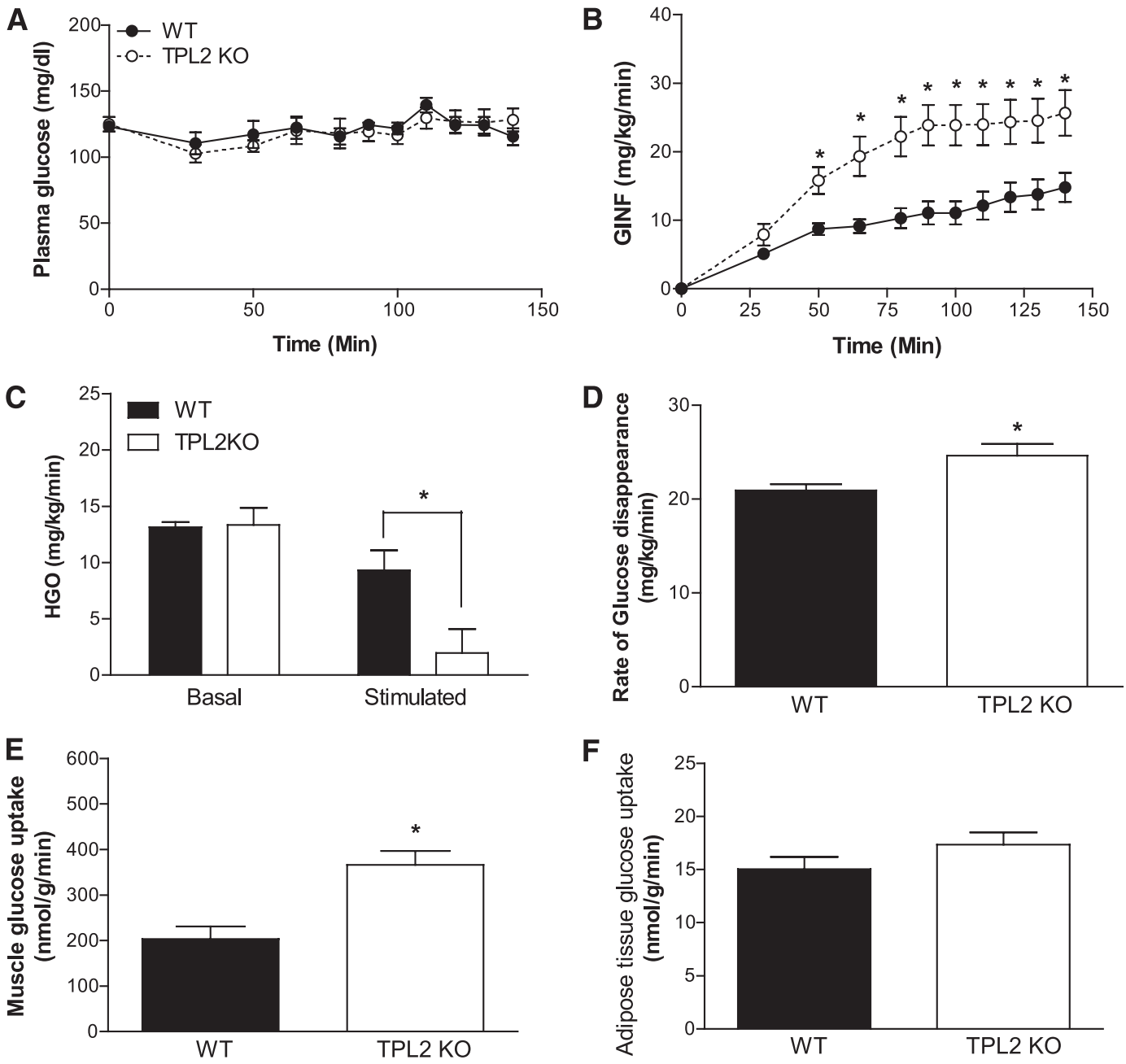

FIG. 6. Hyperinsulinemic-euglycemic clamps revealed that obese TPL2KO mice have an improved insulin sensitivity compared with obese WT mice. *A*: Temporal pattern of plasma glucose concentrations maintained during the hyperinsulinemic-euglycemic clamp. *B*: Steady-state whole-body glucose infusion (GINF) rate during hyperinsulinemic-euglycemic clamps. *C*: Basal and insulin-stimulated hepatic glucose output (HGO). *D*: Rate of glucose disappearance (Rd). *E*: Insulin-stimulated muscle glucose uptake. *F*: Insulin-stimulated white adipose tissue glucose uptake (n = 5–6). *$P < 0.05$. The *error bars* designate the SE.

ACKNOWLEDGMENTS

This work was supported by grants from the American Diabetes Association (R01-DK-082574) to A.S.G.; the Robert C. and Veronica Atkins Foundation Grant to A.S.G.; the U.S. Department of Agriculture, Agricultural Research Service, under agreement No. 58-1950-7-70 to A.S.G.; R01-DK-O74979 to M.S.O.; and in part from T32-DK-007651 to J.W.P., U24-DK-076169 to G.I.S., and R01-DK-40936 to G.I.S. Any opinions, findings, conclusions, or recommendations expressed in this publication are those of the author(s) and do not necessarily reflect the view of the U.S. Department of Agriculture.

No potential conflicts of interest relevant to this article were reported.

J.W.P. and Y.L. researched data and wrote the manuscript. G.I.S. and V.T.S. contributed to discussion and reviewed and edited the manuscript. M.J.J. researched data, contributed to discussion, and reviewed and edited the manuscript. E.C. and C.X. researched data. P.N.T. and M.S.O. contributed to discussion and reviewed and edited the manuscript. A.S.G. wrote the manuscript and contributed to discussion.

The authors thank the following individuals at the JM-USDA Human Nutrition Research Center on Aging at Tufts University: Dr. Don Smith and the CBU staff for their

assistance with care of the animals, and Dr. Katherine Strissel, Dr. Sajid Hussain, and Dr. Victoria Vieira for help with scientific discussion.

REFERENCES

1. Calle EE, Rodriguez C, Walker-Thurmond K, Thun MJ. Overweight, obesity, and mortality from cancer in a prospectively studied cohort of U.S. adults. N Engl J Med 2003;348:1625–1638
2. Hubert HB, Feinleib M, McNamara PM, Castelli WP. Obesity as an independent risk factor for cardiovascular disease: a 26-year follow-up of participants in the Framingham Heart Study. Circulation 1983;67:968–977
3. Fleischman A, Shoelson SE, Bernier R, Goldfine AB. Salsalate improves glycemia and inflammatory parameters in obese young adults. Diabetes Care 2008;31:289–294
4. Weisberg SP, McCann D, Desai M, Rosenbaum M, Leibel RL, Ferrante AW Jr. Obesity is associated with macrophage accumulation in adipose tissue. J Clin Invest 2003;112:1796–1808
5. Xu H, Barnes GT, Yang Q, et al. Chronic inflammation in fat plays a crucial role in the development of obesity-related insulin resistance. J Clin Invest 2003;112:1821–1830
6. Cinti S, Mitchell G, Barbatelli G, et al. Adipocyte death defines macrophage localization and function in adipose tissue of obese mice and humans. J Lipid Res 2005;46:2347–2355
7. Arkan MC, Hevener AL, Greten FR, et al. IKK-beta links inflammation to obesity-induced insulin resistance. Nat Med 2005;11:191–198
8. Hirosumi J, Tuncman G, Chang L, et al. A central role for JNK in obesity and insulin resistance. Nature 2002;420:333–336
9. Yuan M, Konstantopoulos N, Lee J, et al. Reversal of obesity- and diet-induced insulin resistance with salicylates or targeted disruption of Ikkbeta. Science 2001;293:1673–1677
10. Surmi BK, Hasty AH. Macrophage infiltration into adipose tissue: initiation, propagation and remodeling. Future Lipidol 2008;3:545–556
11. Lanthier N, Molendi-Coste O, Horsmans Y, van Rooijen N, Cani PD, Leclercq IA. Kupffer cell activation is a causal factor for hepatic insulin resistance. Am J Physiol Gastrointest Liver Physiol 2010;298:G107–116
12. Huang W, Metlakunta A, Dedousis N, et al. Depletion of liver Kupffer cells prevents the development of diet-induced hepatic steatosis and insulin resistance. Diabetes 2010;59:347–357
13. Strissel KJ, Stancheva Z, Miyoshi H, et al. Adipocyte death, adipose tissue remodeling, and obesity complications. Diabetes 2007;56:2910–2918
14. Griffin ME, Marcucci MJ, Cline GW, et al. Free fatty acid-induced insulin resistance is associated with activation of protein kinase C theta and alterations in the insulin signaling cascade. Diabetes 1999;48:1270–1274
15. Cani PD, Amar J, Iglesias MA, et al. Metabolic endotoxemia initiates obesity and insulin resistance. Diabetes 2007;56:1761–1772
16. Shi H, Kokoeva MV, Inouye K, Tzameli I, Yin H, Flier JS. TLR4 links innate immunity and fatty acid-induced insulin resistance. J Clin Invest 2006;116:3015–3025
17. Patsouris D, Li PP, Thapar D, Chapman J, Olefsky JM, Neels JG. Ablation of CD11c-positive cells normalizes insulin sensitivity in obese insulin resistant animals. Cell Metab 2008;8:301–309
18. Solinas G, Vilcu C, Neels JG, et al. JNK1 in hematopoietically derived cells contributes to diet-induced inflammation and insulin resistance without affecting obesity. Cell Metab 2007;6:386–397
19. De Taeye BM, Novitskaya T, McGuinness OP, et al. Macrophage TNF-alpha contributes to insulin resistance and hepatic steatosis in diet-induced obesity. Am J Physiol Endocrinol Metab 2007;293:E713–E725
20. Cai D, Yuan M, Frantz DF, et al. Local and systemic insulin resistance resulting from hepatic activation of IKK-beta and NF-kappaB. Nat Med 2005;11:183–190
21. Uysal KT, Wiesbrock SM, Marino MW, Hotamisligil GS. Protection from obesity-induced insulin resistance in mice lacking TNF-alpha function. Nature 1997;389:610–614
22. Xiao S, Rose DW, Sasaoka T, et al. Syp (SH-PTP2) is a positive mediator of growth factor-stimulated mitogenic signal transduction. J Biol Chem 1994;269:21244–21248
23. Saberi M, Woods NB, de Luca C, et al. Hematopoietic cell-specific deletion of toll-like receptor 4 ameliorates hepatic and adipose tissue insulin resistance in high-fat-fed mice. Cell Metab 2009;10:419–429
24. Waterfield M, Jin W, Reiley W, Zhang M, Sun SC. IkappaB kinase is an essential component of the Tpl2 signaling pathway. Mol Cell Biol 2004;24:6040–6048
25. Cho J, Melnick M, Solidakis GP, Tsichlis PN. Tpl2 (tumor progression locus 2) phosphorylation at Thr290 is induced by lipopolysaccharide via an Ikappa-B Kinase-beta-dependent pathway and is required for Tpl2 activation by external signals. J Biol Chem 2005;280:20442–20448
26. Das S, Cho J, Lambertz I, et al. Tpl2/cot signals activate ERK, JNK, and NF-kappaB in a cell-type and stimulus-specific manner. J Biol Chem 2005;280:23748–23757
27. Van Acker GJ, Perides G, Weiss ER, Das S, Tsichlis PN, Steer ML. Tumor progression locus-2 is a critical regulator of pancreatic and lung inflammation during acute pancreatitis. J Biol Chem 2007;282:22140–22149
28. Dumitru CD, Ceci JD, Tsatsanis C, et al. TNF-alpha induction by LPS is regulated posttranscriptionally via a Tpl2/ERK-dependent pathway. Cell 2000;103:1071–1083
29. Papoutsopoulou S, Symons A, Tharmalingham T, et al. ABIN-2 is required for optimal activation of Erk MAP kinase in innate immune responses. Nat Immunol 2006;7:606–615
30. Eliopoulos AG, Dumitru CD, Wang CC, Cho J, Tsichlis PN. Induction of COX-2 by LPS in macrophages is regulated by Tpl2-dependent CREB activation signals. EMBO J 2002;21:4831–4840
31. Jager J, Grémeaux T, Gonzalez T, et al. Tpl2 kinase is upregulated in adipose tissue in obesity and may mediate interleukin-1beta and tumor necrosis factor-alpha effects on extracellular signal-regulated kinase activation and lipolysis. Diabetes 2010;59:61–70
32. Nguyen MT, Favelyukis S, Nguyen AK, et al. A subpopulation of macrophages infiltrates hypertrophic adipose tissue and is activated by free fatty acids via Toll-like receptors 2 and 4 and JNK-dependent pathways. J Biol Chem 2007;282:35279–35292
33. Neschen S, Morino K, Hammond LE, et al. Prevention of hepatic steatosis and hepatic insulin resistance in mitochondrial acyl-CoA:glycerol-sn-3-phosphate acyltransferase 1 knockout mice. Cell Metab 2005;2:55–65
34. Rogers NH, Witczak CA, Hirshman MF, Goodyear LJ, Greenberg AS. Estradiol stimulates Akt, AMP-activated protein kinase (AMPK) and TBC1D1/4, but not glucose uptake in rat soleus. Biochem Biophys Res Commun 2009;382:646–650
35. Schwartz DM, Wolins NE. A simple and rapid method to assay triacylglycerol in cells and tissues. J Lipid Res 2007;48:2514–2520
36. Andrikopoulos S, Blair AR, Deluca N, Fam BC, Proietto J. Evaluating the glucose tolerance test in mice. Am J Physiol Endocrinol Metab 2008;295:E1323–E1332
37. Ueki K, Kondo T, Kahn CR. Suppressor of cytokine signaling 1 (SOCS-1) and SOCS-3 cause insulin resistance through inhibition of tyrosine phosphorylation of insulin receptor substrate proteins by discrete mechanisms. Mol Cell Biol 2004;24:5434–5446
38. Rui L, Yuan M, Frantz D, Shoelson S, White MF. SOCS-1 and SOCS-3 block insulin signaling by ubiquitin-mediated degradation of IRS1 and IRS2. J Biol Chem 2002;277:42394–42398
39. Lesniewski LA, Hosch SE, Neels JG, et al. Bone marrow-specific Cap gene deletion protects against high-fat diet-induced insulin resistance. Nat Med 2007;13:455–462
40. Samuel VT, Liu ZX, Wang A, et al. Inhibition of protein kinase Cepsilon prevents hepatic insulin resistance in nonalcoholic fatty liver disease. J Clin Invest 2007;117:739–745
41. Savage DB, Choi CS, Samuel VT, et al. Reversal of diet-induced hepatic steatosis and hepatic insulin resistance by antisense oligonucleotide inhibitors of acetyl-CoA carboxylases 1 and 2. J Clin Invest 2006;116:817–824
42. Carlson CJ, Koterski S, Sciotti RJ, Poccard GB, Rondinone CM. Enhanced basal activation of mitogen-activated protein kinases in adipocytes from type 2 diabetes: potential role of p38 in the downregulation of GLUT4 expression. Diabetes 2003;52:634–641
43. Lumeng CN, Deyoung SM, Bodzin JL, Saltiel AR. Increased inflammatory properties of adipose tissue macrophages recruited during diet-induced obesity. Diabetes 2007;56:16–23
44. Shaul ME, Bennett G, Strissel KJ, Greenberg AS, Obin MS. Dynamic, M2-like remodeling phenotypes of CD11c+ adipose tissue macrophages during high fat diet-induced obesity in mice. Diabetes 2010;59:1171–1181
45. Wu H, Perrard XD, Wang Q, et al. CD11c expression in adipose tissue and blood and its role in diet-induced obesity. Arterioscler Thromb Vasc Biol 2010;30:186–192
46. Lumeng CN, Bodzin JL, Saltiel AR. Obesity induces a phenotypic switch in adipose tissue macrophage polarization. J Clin Invest 2007;117:175–184
47. Watford WT, Wang CC, Tsatsanis C, et al. Ablation of tumor progression locus 2 promotes a type 2 Th cell response in Ovalbumin-immunized mice. J Immunol 2010;184:105–113
48. Banerjee A, Gugasyan R, McMahon M, Gerondakis S. Diverse Toll-like receptors utilize Tpl2 to activate extracellular signal-regulated kinase (ERK) in hemopoietic cells. Proc Natl Acad Sci USA 2006;103:3274–3279
49. Cancello R, Tordjman J, Poitou C, et al. Increased infiltration of macrophages in omental adipose tissue is associated with marked hepatic lesions in morbid human obesity. Diabetes 2006;55:1554–1561